Organic & Biomolecular Chemistry

PAPER

View Article Online
View Journal

Cite this: DOI: 10.1039/c8ob01579a

Reversibly photoswitchable alkoxy azobenzenes connected benzenetricarboxamide discotic liquid crystals with perpetual long range columnar assembly†

Sudha Devi,‡[a] Indu Bala,‡[a] Santosh Prasad Gupta,[b] Pravesh Kumar,[a] Santanu Kumar Pal *[a] and Sugumar Venkataramani *[a]

Liquid crystals (LCs) with photoswitchable groups are very interesting owing to their dual applications. In this regard, we report the synthesis of long chain alkoxy azobenzene incorporated benzenetricarboxamides **7a–c** based room temperature columnar LCs. Apart from the light induced isomerization in the solution phase, the salient feature of these systems is the reversible photoisomerization even in the bulk state with perpetual columnar self-assembly at room temperature. Based on the observation of mesomorphic textures under polarised optical microscopy (POM) and grazing incidence small/wide angle X-ray scattering (GISAXS/GIWAXS) studies, the columnar assembly was found to be stable upon photoisomerization. However, subtle changes in height profile have been observed in AFM measurements after photoswitching. Interestingly, a temperature dependent change between rectangular and hexagonal mesophases in **7a** has been observed. Upon extending the alkoxy chain length, only the hexagonal mesophase was observed. For comparison, the corresponding *N*-methylated derivative of **7a** has also been synthesized. Despite the better photoswitching behaviour, due to the lack of planarity and H-bonding, **8a** did not show any columnar mesophase.

Received 5th July 2018,
Accepted 8th October 2018

DOI: 10.1039/c8ob01579a

rsc.li/obc

Introduction

Recently, there has been increasing interest in discotic liquid crystalline (DLC) materials[1–3] endowed with photoresponsive groups.[4a] These materials have emerged as fascinating functional materials as they combine the optical properties of photochromic groups and self-assembling and dynamic features of DLCs.[4b,c] Photochromic liquid crystals (LCs) are very useful as they can change their mesomorphic state upon irradiation.[5–7] Among the various photochromic groups like spirooxazines, diarylethenes, fulgides *etc.*, azobenzene systems[4b,5–7] are widely studied owing to the rich photochemistry of the azo chromophore and the ease of functionalization at aryl groups.

Besides this, azobenzene based compounds can be very useful in making light modulated switches.[8–10] Tuning of the light induced *E–Z* isomerization channels and the thermal stability of the *Z*-isomer is crucial in making azobenzene based photoswitches.[11–15] Primarily, the structural changes accompanying isomerization provide many opportunities in the design and incorporation of azobenzenes in the molecular systems. Usually, the LC phases of azobenzene incorporated compounds changed to the isotropic phase on irradiation because of the destabilization of the LC phases by *Z*-azobenzene.[16] Particularly, when multiple azobenzenes are introduced through amide linkages, the resulting system can form an interesting supramolecular assembly. The H-bonding reinforced with π–π stacking provides the necessary driving force in this regard. Such systems have found applications in remote-controllable actuators,[6c] photoresponsive surfactants,[17] light induced mass transport[18] *etc.* Lee *et al.* explored the stimulus responsive supramolecular assemblies such as fibers, gels, and spheres using these photoswitchable triamides.[19] Recently, Thiele and co-workers reported the *Z–E* isomerisation processes of multi-state photochromic benzenetricarboxamide systems using *in situ* irradiation NMR spectroscopy.[20] This revealed that the photoisomerization and the reverse

[a]*Department of Chemical Sciences, Indian Institute of Science Education and Research (IISER), Mohali, Sector-81, Knowledge city, Manauli-140306, India. E-mail: skpal@iisermohali.ac.in, sugumarv@iisermohali.ac.in*
[b]*Department of Physics, Patna University, Patna- 800005, India*

†Electronic supplementary information (ESI) available: Detailed synthetic procedure, characterization details, optical microscopy studies, X-ray diffraction studies and photophysical studies. See DOI: 10.1039/c8ob01579a

‡These authors contributed equally.

thermal isomerization processes are not cooperative, and also depend on the concentration.

Furthermore, the utilization of these benzenetricarboxamide cores can create DLCs, due to the well-known behaviour for the formation of columnar mesophases. Hence, in order to find a reliable class of systems, which exhibits LC behaviour at ambient temperature as well as photochromism, we incorporated multiple photochromic groups in our design with alkoxy groups on its periphery. The photochromic moiety is composed of three photoactive azobenzene side groups that are directly linked to a central tricarboxamide benzene core (Scheme 1). Herein, we reported the investigations on the LC properties of these systems and also their photoswitching behaviour in solution as well as in the LC form.

Synthesis of target molecules 7a–c/8a

The target molecules **7a–c**/**8a** have been synthesized using 4-aminoacetanilide **1** as the starting material (Scheme 1). Compound **1** has been diazotized and treated with phenol to obtain the hydroxyazobenzene derivative **2** as per the literature procedure.[21] In order to obtain the ethers **3a–c**, *O*-alkylation has been performed with different alkyl bromides (*n*-hexyl, *n*-octyl and *n*-decyl bromides) using potassium carbonate as a base in the presence of a catalytic quantity of potassium iodide. Without purification of the acetanilide derivatives **3a–c**, they were subjected to acid hydrolysis, which led to their corresponding amine products **4a–c** in good yields. The *N*-methylated **4a-NMe** derivative was synthesized by reductive methylation using **3a**, formaldehyde and sodium cyanoborohydride at 0 °C. Finally, the *in situ* generated trimesoyl chloride **6** has been used to react with the amine compounds **4a–c** to obtain the corresponding triamide target molecules **7a–c**. In a similar way, the *N*-methylated derivative **8a** has been synthesized using **4a-NMe**. The detailed synthetic procedures for all the compounds are described in the ESI.† All the intermediates and the target molecules have been characterized by ^{1}H, ^{13}C-NMR, IR, UV-Vis and HRMS spectral techniques (Fig. S12–S32, see the ESI†).

Analysis of photoswitching behaviour of 7a–c/8a by using UV-Vis and NMR (in solution state)

The photoswitching behaviour of all the target molecules **7a–c** and the *N*-methylated derivative **8a** has been studied in the solution phase ($CHCl_3$ and DMSO) and analysed by UV-Vis spectroscopy (Fig. 1, S1–S5, see the ESI†). The photoswitching in the solid state for **7a** (*vide infra*) and **8a** (Fig. S6, see the ESI†) has been carried out at room temperature. Additionally, the analysis of photoswitching behaviour has also been carried out using an NMR spectroscopic technique. Upon irradiation at 365 nm light, the molecules isomerize to all-*cis* configuration, inferred from the spectral changes in the π–π* and n–π* absorptions. All the three target compounds showed almost identical absorption spectra for both before and after switching. The absence of spectral changes clearly indicated that the chain length did not perturb the absorption spectra of all the three molecules at all. To envisage the thermal stability of the resulting isomer, kinetics has been followed for all the three isomers (Fig. S9–S11, see the ESI†). The net rate of formation of **7a–c**-*EEE* is found to decrease upon increasing the alkyl chain length (Fig. S9–S11,† Table 1). Similarly the *N*-methylated **8a** has also been subjected to photoswitching. Under comparable concentration in $CHCl_3$, **8a** showed a fast photoswitching leading to all-*cis* isomer; however, the reverse isomerization did not happen even after prolonged irradiation at different wavelengths. In contrast, the DMSO solution of **8a** showed almost quantitative reverse photoswitching at 505 nm. Since UV-Vis spectroscopy is unable to differentiate among the

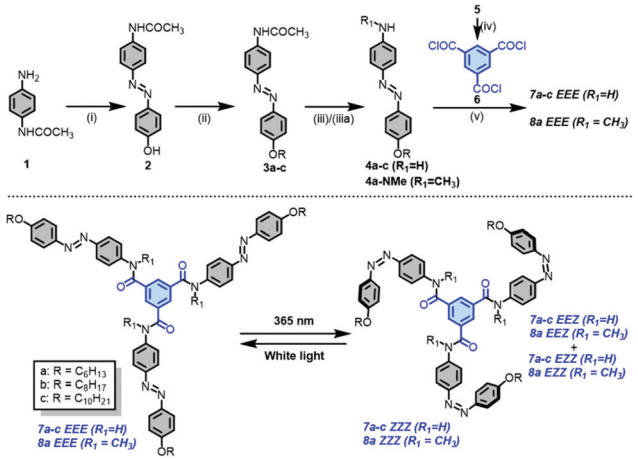

Scheme 1 Synthesis of target compounds **7a–c**/**8a** and their photoisomerization channel. (i) Conc. HCl, $NaNO_2$, phenol, aq. NaOAc, 0 °C, 4 h, 91%; (ii) K_2CO_3, R-Br, cat. KI, dry DMF, 100 °C, 6–8 h; (iii) conc. HCl, EtOH, reflux, 5–6 h, **4a**-82%, **4b**-84%, **4c**-84%; (iiia) for **4a-NMe**: formaldehyde, $NaCNBH_3$, MeOH, 0 °C, 2 h, 32%; (iv) trimesic acid (**5**), PCl_5, toluene, reflux; (v) pyridine, toluene, RT, 4–5 h, **7a**-76%, **7b**-72%, **7c**-75%, **8a**-40%.

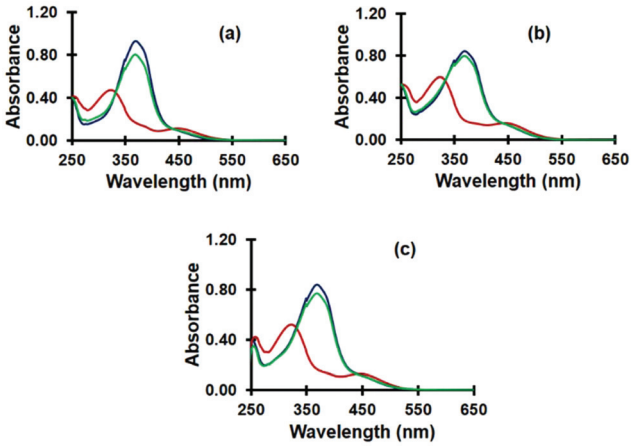

Fig. 1 Analysis of photoswitching behaviour using UV-Vis spectroscopy for the target molecules: (a) **7a** (9.6 μM); (b) **7b** (9.5 μM); (c) **7c** (8.2 μM). All the spectra are recorded in $CHCl_3$; spectral colour scheme: blue – spectra of **7a–c**-*EEE*; red – spectra recorded after irradiation at 365 nm; green – spectra recorded after reverse switching using white light (32 W CFL lamp).

Table 1 Absorption spectral properties and solution phase formation rate constants of **7a–c**-*EEE* using UV-Vis spectroscopy

TM	$\lambda_{max}/(\varepsilon)^a$ (*EEE*)	$\lambda_{max}{}^{a,b}$	k (x10^{-5})^c	Half life^c
7a^d	**369 (75 058 ± 152)**	**323, 446**		
	375	320, 448	2.82	410
7b	**369 (83 663 ± 312)**	**323, 446**		
	375	320, 448	4.00	286
7c	**369 (84 613 ± 42)**	**323, 446**		
	375	320, 448	4.32	267

^{a} λ_{max} values (nm) and ε values in parentheses (L mol^{-1} cm^{-1}) of **7a–c**-*EEE*; bold – in $CHCl_3$ and normal font – in DMSO. ^{b} After 365 nm irradiation. ^{c} Rate constants (min^{-1}) and the half-lives (min) have been measured in DMSO at 25 ± 1 °C; abbreviation: TM – target molecules. ^{d} For **7a**, the absorption maxima in the solid state and LC state were observed at 377 nm and 372 nm, respectively.[22]

three individual isomers (*EEZ*, *EZZ* and *ZZZ*-isomers), we shifted our attention to NMR spectroscopy for understanding their presence (Fig. 2, Fig. S7, see the ESI†). The NMR spectra of target compounds recorded in DMSO-d$_6$ showed well-resolved and sharp signals. Besides that, we also observed the formation of a photostationary state (PSS) upon irradiation at 365 nm, where all the four species coexist (Fig. 1). Based on the spectral changes, we observed that upon *E* to *Z* isomerization, the signals were found to be shifted to the upfield region. Due to their non-overlapping nature, the aromatic benzene core protons (appearing as a singlet in *EEE*-isomer) have been used for identifying the individual isomers. Also, the signals clearly showed a progressive upfield shift as a result of gaining more *Z*-configuration. At the PSS corresponding to 365 nm, the major species was found to be *ZZZ*-isomer, which showed a maximum upfield shift of the benzene core protons. The appearance of signals with 1 : 2 and 2 : 1 integral ratios has been used to differentiate between the *EEZ* and *ZZE*-isomers. Based on the photoswitching studies, it is clear that maximum *ZZZ*-isomer conversion (64%) can be achieved at 14.1 mM concentration. Again, the photoswitching studies on the *N*-methylated **8a** have also been carried out in DMSO-d$_6$. The forward switching at 365 nm led to almost quantitative conversion into all-*cis* isomer; however, even after continuous irradiation, the reverse isomerization was found to be incomplete. Due to the overlapping signals, the identification of composition of various isomers was difficult (Fig. S8, see the ESI†).

Thermal behaviour of 7a–c/8a

The thermal behaviour of the newly synthesized tris-azobenzenetricarboxamide series was first studied by polarized optical microscopy. All the compounds were found to exhibit LC behaviour at room temperature. Under POM, compound **7a** exhibited LC behaviour at room temperature and melted into an isotropic liquid at 238.0 °C. On cooling from its isotropic melt, it exhibited a needle like texture consisting of rectilinear defects and homeotropic domains (Fig. 3b) indicating the Col$_h$ mesophase. Then it transformed into a four brush texture (Fig. 3a) at 160.4 °C, a representative of the Col$_r$ mesophase, which then stayed up to room temperature. Compound **7b** exhibited mostly homeotropically aligned textures which on pressing (top of the glass slide) gives isogyre type textures (Fig. 3c), and further phase confirmation led to the existence of the Col$_h$ phase as predicted by the X-ray diffraction (XRD) technique (*vide infra*). And also, on shearing in one direction, the compound formed homogeneous domains, a characteristic of LCs (Fig. 3d).

In differential scanning calorimetry (DSC), it displayed a mesophase to isotropic transition at 190 °C, while on cooling it showed no observable transition, which may be due to low enthalpy changes. Similar to **7b**, compound **7c** also exhibited a birefringent texture along with rectilinear defects in some areas, a characteristic of the Col$_h$ phase (Fig. 3e). And on heating, it showed the mesophase to isotropic transition at 175 °C. The phase transition temperatures for all the com-

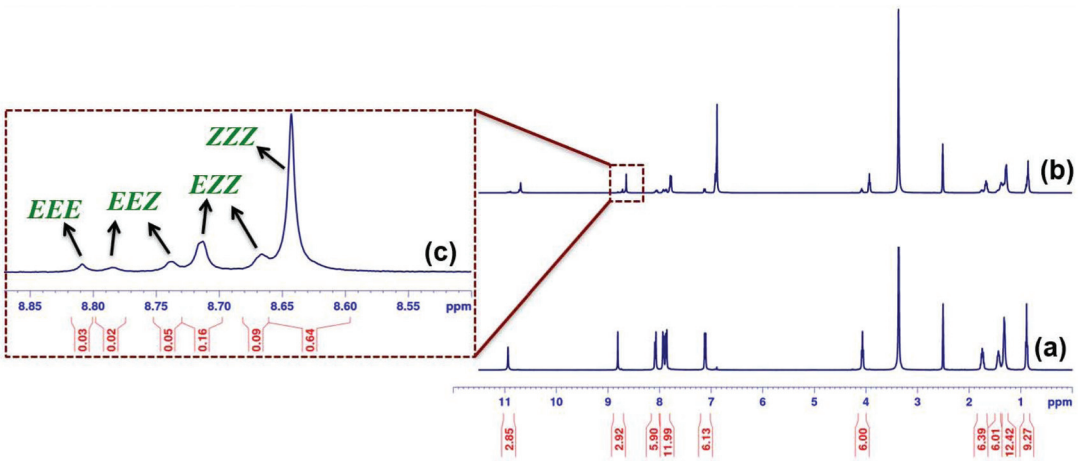

Fig. 2 ^{1}H NMR spectra corresponding to: (a) **7a**-*EEE* as a 14.1 mM concentration solution in DMSO-d$_6$; (b) the same solution after being subjected to irradiation at 365 nm for 130 min; (c) the expanded region depicts the benzene core protons in "b" with the indication of normalized integral values corresponding to *EEE*, *EEZ*, *EZZ* and *ZZZ* isomers of **7a**.

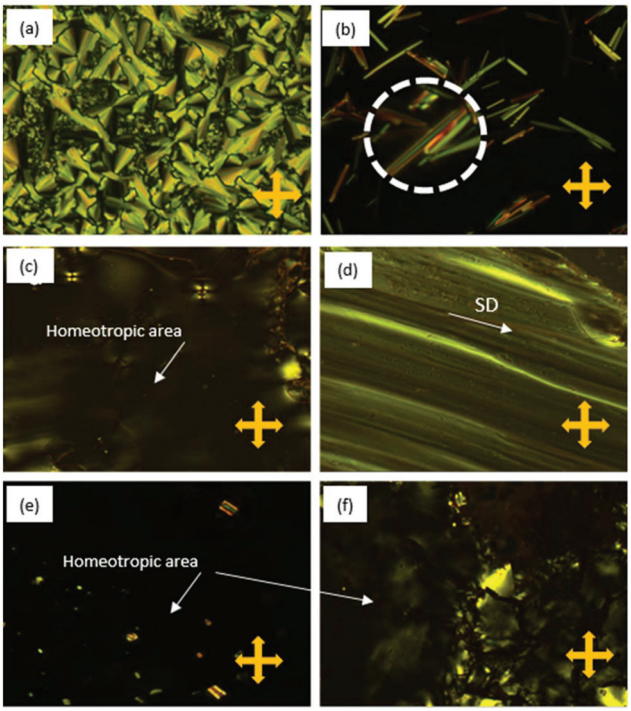

Fig. 3 Photomicrographs: (a) compound **7a** at 120 °C (Col_r, ×500); (b) at 220 °C (Col_h, ×500); (c) **7b** at 68.6 °C (Col_h, ×100); (d) **7b** on shearing at room temperature (Col_h, ×100); (e) **7c** at 69.2 °C; (Col_h, ×500); (f) **7c** at 35.2 °C (×200), observed on cooling from isotropic liquid with a scan rate of 5 °C min^{-1}.

Table 2 Thermal behaviour[a] of the target compounds **7a–c**

TM	Heating	Cooling
7a	Col_r 165 Col_h 238 Iso[b]	Iso 230 Col_h 160.4 Col_r [b]
7b	Col_h 190 Iso[c]	Iso 185 Col_h [b]
7c	Col_h 175 Iso[c]	Iso 165 Col_h [b]

[a] Phase transition temperature (°C). [b] Transition temperature from POM. [c] Transition temperature from DSC. Abbreviations: TM = target molecules, Col_r = columnar rectangular, Col_h = columnar hexagonal, Iso = isotropic liquid.

pounds are listed in Table 2. So, all the compounds exhibited enantiotropic mesomorphic behaviour as very well observed by POM and X-ray studies, however, some of the transitions were not observed in DSC probably due to the low enthalpy change associated with the transitions as reported earlier.[23a,24,25] As expected, the *N*-methylated derivative **8a** did not show any specific texture corresponding to the columnar mesophase (data not shown) plausibly due to the absence of intermolecular H-bonding and lack of planarity.[26] Furthermore, the XRD measurement of **8a** showed a weak but broad peak at a small angle, which is contrary to the **7a–c** derivatives (exhibiting sharp peaks in the small angle regions). This indicates the absence of columnar order in **8a** (*i.e.* the structure is more random). We have also checked the possibility of decomposition in compound **8a** upon melting (mp 185 °C) prior to filling it in the capillary for XRD measurements. The NMR spectral data for the heated sample of **8a** confirmed no decomposition upon melting.

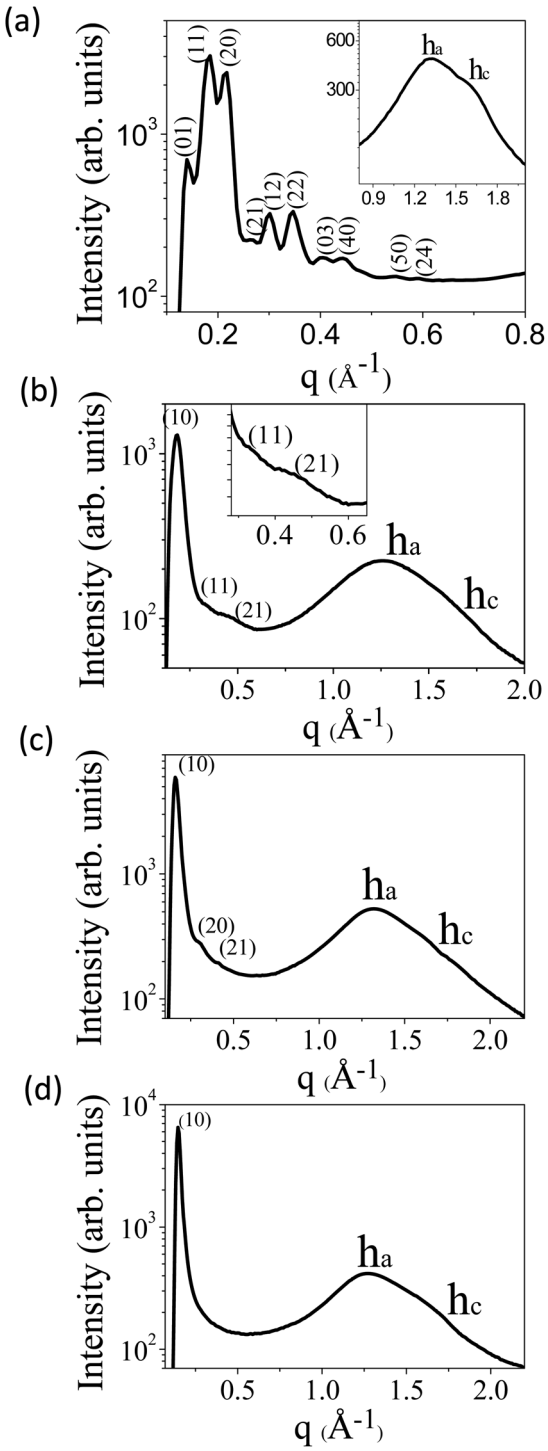

Fig. 4 X-ray diffraction pattern: (a) compound **7a** in Col_r at 140 °C; (b) compound **7a** in Col_h at 190 °C; (c) compound **7b** in Col_h at 25 °C; (d) compound **7c** in Col_h at 115 °C, obtained on cooling from the isotropic liquid, h_a and h_c are the spacings appearing due to alkyl chain–chain and core–core correlation, respectively.

XRD experiments were performed to deduce the exact structure of the assembly of the mesophases. Compound **7a** at lower temperature, in the range of 25 to 160 °C, exhibited many peaks in the small angle region. In addition, there were h_a and h_c peaks in the wide-angle region. The h_a peak mainly originated due to the liquid like order of the fluid chain and the h_c peak appears due to the core–core separation and it is indicative of π–π interaction, reflecting the columnar nature of the mesophase (Fig. 4a). The peaks of the small angle could be indexed on the rectangular lattice. The calculated 2D lattice parameters are a = 57.20 Å and b = 44.84 Å (at 140 °C). The h_c peak sets the value of the other lattice parameter *i.e.* c = 3.89 Å (Table 3). In brief, the observed phase is Col_r. Furthermore, this phase transformed into the Col_h phase at a temperature of 160.4 °C, and persisted in the temperature range of 160.4 to 238 °C. The phase is confirmed by the observation of three peaks in the ratio of $1 : 1/\sqrt{3} : 1/\sqrt{7}$ which correspond to the reflections from the (10), (11) and (21) planes, respectively, of the hexagonal lattice (Fig. 4b and Table 3). Furthermore, h_a and h_c peaks were also observed in the wide-angle region where the h_c peak confirmed its columnar nature. The calculated lattice parameter was found to be a = 39.24 Å and the other lattice parameter was set by the value of the spacing of the h_c peak (c = 3.62 Å).

In summary, compound **7a** exhibits the Col_r phase at lower temperature (25–160 °C) and the Col_h phase at higher temperature (160.4–238 °C). This phase behaviour has also been well supported by POM studies. In contrast, compounds **7b** and **7c** showed only Col_h phase (Fig. 4c & d). Hence, the Col_h to Col_r phase transition occurs on increasing the temperature as in **7a** (Fig. 5) and also on increasing the peripheral alkoxy chain length on going from **7a** to **7c**. The lattice parameters are found to be a = 43.35 Å and 49.74 Å (Table 3), respectively, which reflect the increasing trend. This trend is obvious because the periphery chain length (size of the molecule) is increasing from compound **7a** to **7c**.

Reconstructed electron density maps (EDM)

Electron density maps for the Col_r and Col_h phase of compound **7a** were reconstructed (Fig. 6a and b). The procedure to reconstruct the electron density map has been described in the earlier literature.[23,25] The peak intensities and their phase values were obtained to reconstruct the maps. The details (multiplicity and phase values) are given in Table 3.

Photoswitching studies in solid state

After confirming the mesomorphic properties of all the three molecules, we focused on the photoswitching behaviour in the solid state. In this regard, the solid-state photoswitching of **7a** has been studied in KBr using UV-Vis spectroscopy (Fig. 7a). The spectral changes upon irradiation at 365 nm clearly indicated the isomerization process. Molecule **7a** also exhibited the photoswitching in thin film, however, with a slight blue shift in the π–π* absorption bands (Fig. S33, see the ESI†).

Table 3 The indices, observed and calculated d-spacings and planes of the diffraction peaks of the lattices

TM	Mesophase	Lattice constants (Å)	d_{obs} [a] (Å)	d_{cal} [b] (Å)	MI	RI (M)
7a	Col_h at 140 °C	a = 57.20	44.78	44.84	01	22.91(2)
		b = 44.84	35.16	35.29	11	100.00(4)
		c = 3.89	28.91	2.60	20	78.84(2)
			23.90	24.11	21	7.34(2)
			20.83	20.87	12	10.64(4)
			17.93	17.65	22	10.98(4)
			15.28	14.95	03	5.72(2)
			14.14	14.30	40	5.65(2)
			11.46	11.44	50	4.33(2)
			10.59	10.44	24	4.26(4)
			9.93	9.66	34	4.16(4)
			9.54	9.53	60	4.16(2)
			4.81		h_a	
			3.80		h_c	
	Col_h at 190 °C	a = 39.24	33.99	33.17	10	
		c = 3.62	19.57	19.15	11	
			13.15	8.93	21	
			4.95	4.89	h_a	
			3.62	3.88	h_c	
7b	Col_h at 25 °C	a = 45.47	39.38	39.38	10	
		c = 3.88	19.89	19.69	20	
			15.14	14.88	21	
			4.79		h_a	
					h_c	
7c	Col_h at 115 °C	a = 49.76	43.09	43.09	10	
		c = 3.62	4.94		h_a	

[a] d_{obs}: Experimental d-spacing. [b] d_{cal}: Calculated d-spacing for Col_r by using the relation: $\frac{1}{d^2} = \left[\frac{h^2}{a^2} + \frac{k^2}{b^2}\right]$; for Col_h: $\frac{1}{d^2} = \left[\frac{4}{3}\left(\frac{h^2 + hk + k^2}{a^2}\right) + \frac{l^2}{c^2}\right]$; h, k, and l are the indices of the reflections corresponding to the columnar hexagonal (Col_h) phase; a & c are the unit cell parameters, h_a & h_c spacing appear due to alkyl chain–chain and core–core correlation, respectively. Abbreviation: TM – target molecules, MI – Miller indices, RI (M) – relative intensity (multiplicity).

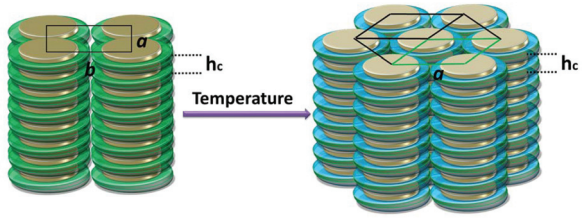

Fig. 5 Model representing temperature induced Col_r to Col_h transition in **7a**.

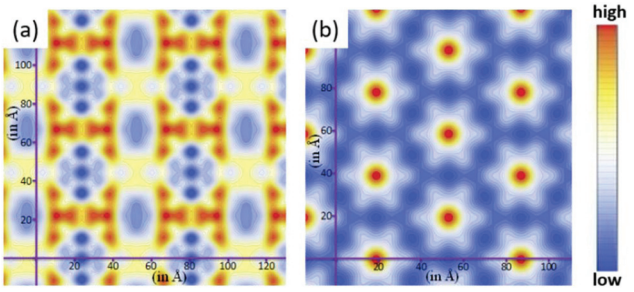

Fig. 6 (a) Reconstructed electron density map of columnar rectangular (Col_r) and (b) columnar hexagonal (Col_h) phases. Red represents the highest electron density and deep blue is the lowest.

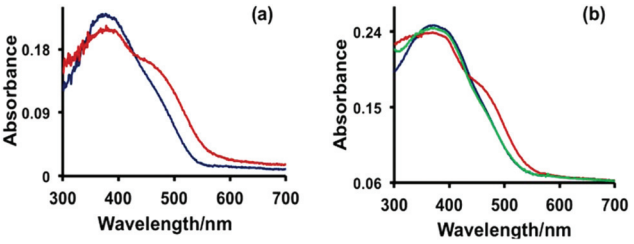

Fig. 7 Photoswitching behaviour in the solid state for **7a**: (a) in KBr; (b) in the thin film LC state. The blue coloured spectrum is due to **7a**-*EEE* (before irradiation), whereas the red one indicates the changes after irradiation at 365 nm. The spectra appearing in green in "b" was observed after reverse switching on heating.

Furthermore, we also considered the photoswitching studies in its LC state (Fig. 7b). In this regard, compound **7a** was first heated to its isotropic temperature and then cooled back to room temperature LC state as observed through POM. Then the same sample has been subjected to photoswitching and monitored by UV-Vis spectroscopic studies. On irradiating the sample with 365 nm UV light, the compound exhibited characteristic changes accompanying the *E*–*Z* isomerization. Interestingly, the sample reverted to its native configuration upon heating that can be rationalized from the changes in the n–π* absorption. This clearly demonstrates the reversible photoswitching of molecule **7a** in the LC form. Nevertheless, POM studies of the samples in the LC form showed that both the samples (before and after irradiation at 365 nm) exhibited identical images. Despite a prolonged irradiation using 365 nm light, the sample retained the texture without exhibiting any appreciable change in the mesophase (Fig. S34a and b, see the ESI†). This indicates that the columnar self-assembly was unperturbed upon photoisomerisation (Fig. 8c). Presumably, the attachment of azobenzene moieties to a rigid benzene tricarboxamide core provides too tight packing to change the molecular self-assembly upon isomerization. The structure in which the rigid core is attached to azobenzene units *via* flexible alkyl spacers is more effective in changing the columnar self-assembly as reported earlier.[27] To further see the change in the columnar self-assembly upon UV irradiation, GISAXS/GIWAXS studies were carried out on thin films of **7a** (Fig. S34c–f, see the ESI†). Similarly, the GISAXS/GIWAXS patterns were unaltered before and after irradiation as shown in Fig. S34 (see the ESI†). All this experimental evidence clearly envisage the possibility of photoswitching in these target molecules without affecting their supramolecular assembly.

Furthermore, the atomic force microscopy (AFM) measurements of the dropcast sample of **7a** in HPLC grade dichloromethane were performed on a glass substrate (Fig. 8a & b, Fig. S35, see the ESI†). We monitored the changes in the morphology of the thin film before and after irradiating the sample for 30 minutes with 365 nm UV light. As suggested by an earlier report, the disturbance or changes in the columnar assembly can alter the height profile.[27] However, we observed only subtle changes in the height profile that indicate the

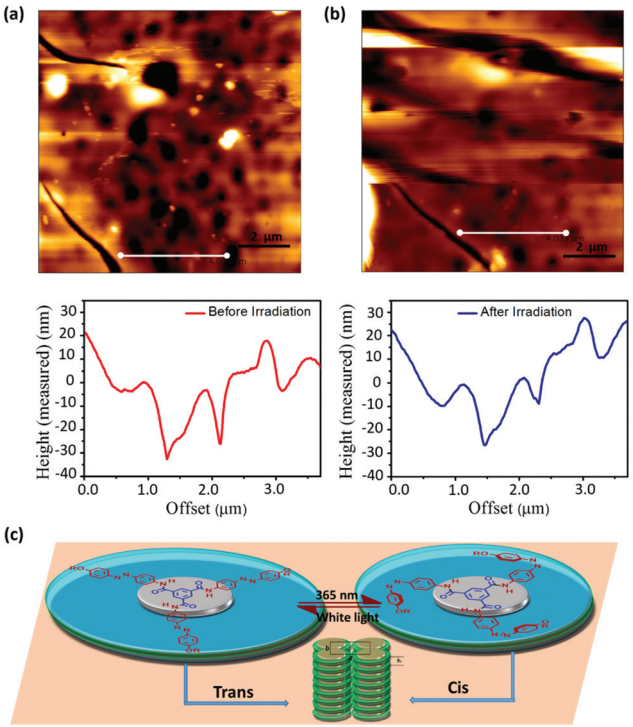

Fig. 8 AFM images of dropcast film of **7a** on a glass substrate: (a) before irradiation; (b) after irradiation. (c) Schematic showing columnar assembly retains upon reversible photoisomerization. Note: All the photoswitching studies were carried out at room temperature.

retention of columnar self-assembly during photoisomerization.

Conclusions

In conclusion, we have synthesized three long chain alkoxy azobenzene connected benzenetricarboxamide derivatives. All the three molecules are found to behave as discotic liquid crystals. Interestingly, the molecule with a peripheral C_6 alkyl chain exhibits temperature dependent changes in the mesophases. A Col_r phase was observed at low temperature, whereas, a Col_h at higher temperature was seen. The other two higher homologues revealed only Col_h phases at all temperature ranges. All the three molecules showed solution state photoswitching. At the μM concentration range, all the three molecules showed nearly complete photoswitching, however, at a higher concentration (mM range), NMR spectroscopy predicted a partial isomerization with the coexistence of all four possible isomers at the photostationary state. Significant photoswitching was also observed in the solid state and LC phase however, without changing its supramolecular assembly, which was also supported by AFM and POM studies. For comparison, an *N*-methylated analogue **8a** has been synthesized and studied for the columnar mesomorphic behaviour. However, due to the lack of H-bonding and planarity, it did not exhibit any mesophases despite having better photoswitching behaviour. Thus, the tris-azobenzenetricarboxamide based systems are found to be versatile DLCs exhibiting reversible photoswitching behavior without losing their LC properties upon isomerization.

Conflicts of interest

There are no conflicts to declare.

Acknowledgements

SV is grateful to the SERB, New Delhi for the financial support (EMR/2014/000780). We are thankful to the IISER Mohali for the NMR, HRMS, SAXS/WAXS and other instrumentation facilities and also for providing the start-up grant. We are thankful to C. Sai Srinivas and Dr Sabyasachi Rakshit for AFM studies. SD thanks the UGC for Junior and Senior Research Fellowships. IB and PK acknowledge the CSIR (09/947(0061/2015-EMR-1 and 09/947(0077/2016-EMR-1, respectively) for fellowships. Dr SK Pal acknowledges funding from CSIR (02(0311)/17/EMR-II).

References

1 (*a*) S. Kumar, *Chem. Soc. Rev.*, 2006, **35**, 83; (*b*) S. Kumar, *Liq. Cryst.*, 2004, **31**, 1037.
2 A. N. Cammidge and R. J. Bushby, in *Handbook of Liquid Crystals*, ed. D. Demus, J. W. Goodby, G. W. Gray, H. W. Spiess and V. Vill, Wiley- WCH, Weinheim, 1998, vol. 7, p. 693.
3 (*a*) R. J. Bushby and K. Kawata, *Liq. Cryst.*, 2011, **38**, 1415; (*b*) T. Wohrle, I. Wurzbach, J. Kirres, A. Kostidou, N. Kapernaum, J. Litterscheidt, J. C. Haenle, P. Staffeld, A. Baro, F. Giesselmann and S. Laschat, *Chem. Rev.*, 2016, **116**, 1139.
4 (*a*) K. Ichimura, S. Furumi, S. Y. Morino, M. Kidowaki, M. Nakagawa, M. Ogawa and Y. Nishiura, *Adv. Mater.*, 2000, **12**, 950; (*b*) H. K. Bisoyi and Q. Li, *Chem. Rev.*, 2016, **116**, 15089; (*c*) M. Alaasar, S. Poppe, Q. Dong, F. Liu and C. Tschierske, *Angew. Chem., Int. Ed.*, 2017, **56**, 10801.
5 (*a*) M. Frigoli and G. H. Mehl, *Chem. Commun.*, 2004, 2040; (*b*) M. Irie, *Chem. Rev.*, 2000, **100**, 1685; (*c*) M. Frigoli and G. H. Mehl, *J. Org. Chem.*, 2004, 636; (*d*) M. Frigoli and G. H. Mehl, *Mol. Cryst. Liq. Cryst.*, 2005, **430**, 123; (*e*) A. Zep, M. M. Wojcik, W. Lewandowski, K. Sitkowska, A. Prominski, J. Mieczkowski, D. Pociecha and E. Gorecka, *Angew. Chem., Int. Ed.*, 2014, **53**, 13725.
6 (*a*) Y. Chen, W. T. Harrison, C. T. Imrie and K. S. Ryder, *J. Mater. Chem.*, 2002, **12**, 579; (*b*) Q. Li, J. Kim, H. S. Park and J. Williams, *Chem. Mater.*, 2005, **17**, 6018–6021; (*c*) Y.-J. Choi, D.-Y. Kim, M. Park, W.-J. Yoon, Y. Lee, J.-K. Hwang, Y.-W. Chiang, S.-W. Kuo, C.-H. Hsu and K.-U. Jeong, *ACS Appl. Mater. Interfaces*, 2016, **8**, 9490; (*d*) S. Pan, M. Ni, B. Mu, Q. Li, X.-Y. Hu, C. Lin, D. Chen and L. Wang, *Adv. Funct. Mater.*, 2015, **25**, 3571.
7 (*a*) J. H. Sung, S. Hirano, O. Tsutsumi, A. Kanazawa, T. Shiono and T. Ikeda, *Chem. Mater.*, 2002, **14**, 385; (*b*) H. Adachi, Y. Hirai, T. Ikeda, M. Maeda, R. Hori, S. Kutsumizu and T. Haino, *Org. Lett.*, 2016, **18**, 924; (*c*) K. Kreger, P. Wolfer, H. Audorff, L. Kador, N. Stingelin-Stutzmann, P. Smith and H.-W. Schmidt, *J. Am. Chem. Soc.*, 2010, **132**, 509.
8 (*a*) C. Dugave and L. Demange, *Chem. Rev.*, 2003, **103**, 2475–2532; (*b*) J. Garcia-Amoros and D. Velasco, *Beilstein J. Org. Chem.*, 2012, **8**, 1003.
9 (*a*) S. Kobatake, S. Takami, H. Muto, T. Ishikawa and M. Irie, *Nature*, 2007, **446**, 778; (*b*) S. Guo, K. Matsukawa, T. Miyata, T. Okubo, K. Kuroda and A. Shimojima, *J. Am. Chem. Soc.*, 2015, **137**, 15434.
10 (*a*) J. Henzl, M. Mehlhorn, H. Gawronski, K.-H. Rieder and K. Morgenstern, *Angew. Chem., Int. Ed.*, 2006, **45**, 603; (*b*) A. A. Beharry and G. A. Woolley, *Chem. Soc. Rev.*, 2011, **40**, 4422; (*c*) S. Devi, A. K. Gaur, D. Gupta, M. Saraswat and S. Venkataramani, *ChemPhotoChem*, 2018, **2**, 806.
11 H. M. D. Bandara and S. C. Burdette, *Chem. Soc. Rev.*, 2012, **41**, 1809.
12 X. Xia, H. Yu, L. Wang and Z. ul-Abdin, *RSC Adv.*, 2016, **6**, 105296.
13 O. Kulikovska, L. M. Goldenberg and J. Stumpe, *Chem. Mater.*, 2007, **19**, 3343.
14 J. Ge and Y. Yin, *Angew. Chem., Int. Ed.*, 2011, **50**, 1492.

15 S. Guo, K. Matsukawa, T. Miyata, T. Okubo, K. Kuroda and A. Shimojima, *J. Am. Chem. Soc.*, 2015, **137**, 15434.
16 M. Pfletscher, C. Wölper, J. S. Gutmann, M. Mezger and M. Giese, *Chem. Commun.*, 2016, **52**, 8549.
17 Y. Huang and D.-H. Kim, *Nanoscale*, 2012, **4**, 6312.
18 L. M. Goldenberg, L. Kulikovsky, O. Kulikovska, J. Tomczyk and J. Stumpe, *Langmuir*, 2010, **26**, 2214.
19 S. Lee, S. Oh, J. Lee, Y. Malpani, Y.-S. Jung, B. Kang, J. Y. Lee, K. Ozasa, T. Isoshima, S. Y. Lee, M. Hara, D. Hashizume and J.-M. Kim, *Langmuir*, 2013, **29**, 5869.
20 J. Kind, L. Kaltschnee, M. Leyendecker and C. M. Thiele, *Chem. Commun.*, 2016, **52**, 12506.
21 I. Carlescu, A. M. Scutaru, D. Apreutesei, V. Alupei and D. Scutaru, *Liq. Cryst.*, 2007, **34**, 775.
22 The UV-Vis spectra of **7a-*EEE*** in the solid state and the LC state showed strong features corresponding to the π–π* absorption. Upon irradiation at 365 nm, we observed the changes in π–π* as well as in n–π* absorptions. Unlike the solution phase absorption spectral changes, the new features appeared as a shoulder, and so the maxima corresponding to π–π* and n–π* could not be predicted clearly.
23 (*a*) I. Bala, S. P. Gupta, J. De and S. K. Pal, *Chem. – Eur. J.*, 2017, **23**, 12767; (*b*) S. P. Gupta, M. Gupta and S. K. Pal, *ChemistrySelect*, 2017, **2**, 6070.
24 J. Luo, B. Zhao, H. S. O. Chan and C. Chi, *J. Mater. Chem.*, 2010, **20**, 1932.
25 (*a*) J. De, S. P. Gupta, I. Bala, S. Kumar and S. K. Pal, *Langmuir*, 2017, **33**, 13849; (*b*) I. Bala, H. Singh, V. R. Battula, S. P. Gupta, J. De, S. Kumar, K. Kailasam and S. K. Pal, *Chem. – Eur. J.*, 2017, **23**, 14718.
26 (*a*) I. Azumaya, H. Kagechika, K. Yamaguchi and K. Shudo, *Tetrahedron*, 1995, **51**, 5277; (*b*) F. D. Lewis, T. M. Long, C. L. Stern and W. Liu, *J. Phys. Chem. A*, 2003, **107**, 3254; (*c*) K. Pandurangan, J. A. Kitchen, S. Blasco, E. M. Boyle, B. Fitzpatrick, M. Feeney, P. E. Kruger and T. Gunnlaugsson, *Angew. Chem., Int. Ed.*, 2015, **127**, 4649.
27 D. Tanaka, H. Ishiguro, Y. Shimizu and K. Uchida, *J. Mater. Chem.*, 2012, **22**, 25065.

